Electronic Supplementary Material (ESI) for Lab on a Chip.

Supporting Information

Railing Cells along 3D Microelectrode Tracks for a Continuous-Flow Dielectrophoretic Sorting

Xiaoxing Xing,[ab] *Chun Ning Ng,*[c] *Ming Lok Chau,*[b] *and Levent Yobas*[*bc]

[a]College of Information Science and Technology, Beijing University of Chemical Technology, Beijing 100029, China

[b]Dept. of Electronic and Computer Engineering, The Hong Kong University of Science and Technology, Clear Water Bay, Hong Kong SAR, China. Email: eelyobas@ust.hk

[c]Division of Biomedical Engineering, The Hong Kong University of Science and Technology, Clear Water Bay, Hong Kong SAR, China.

[*]E-mail: eelyobas@ust.hk

Contents:

THEORY

Dielectrophoretic force is vital in docking and retaining cells along the tracks, and often has to work against hydrodynamic drag. These two forces, however, must be proportional for an effective cell railing. Excessive pDEP may trap cells around the field maxima whereas rather weak pDEP is unlikely to achieve cell docking and/or retaining cells along the tracks. Moderately strong pDEP can modulate the railing speed due to the wavy layout of the track, alternatingly accelerating and decelerating cells. Time-averaged DEP force exerted by a non-uniform electric field $\bar{E}$ on a spherical particle suspended in a medium can be expressed as:[1]

$$\langle \bar{F}_{DEP} \rangle = 2\pi\varepsilon_m R^3 \mathrm{Re}[f_{CM}(\omega)] \nabla(|\bar{E}|^2) \quad \text{(S–1)}$$

where ε_m is the absolute permittivity of the medium, R the particle radius, ∇ the vector differential (del) operator, $\omega = 2\pi f$ the activation angular frequency with f being the ordinary frequency, and $\mathrm{Re}[f_{CM}(\omega)]$ the real part of the Clausius-Mossotti (CM) factor. The CM factor compares the particle complex permittivity ε_p^* to that of the medium ε_m^*:

$$f_{CM}(\omega) = \frac{\varepsilon_p^* - \varepsilon_m^*}{\varepsilon_p^* + 2\varepsilon_m^*} \quad \text{(S–2)}$$

A complex permittivity ε_i^* is such that $\varepsilon_i^* = \varepsilon_i - j\sigma_i/\omega$, with ε_i and σ_i, the absolute permittivity and conductivity of the material denoted by the subscript i. The sign of $\mathrm{Re}[f_{CM}(\omega)]$ sets the polarity and direction of the DEP force: pDEP for $\mathrm{Re}[f_{CM}(\omega)] > 0$, and nDEP for $\mathrm{Re}[f_{CM}(\omega)] < 0$. The switch in polarity occurs at a so-called crossover frequency ω_c, where $\mathrm{Re}[f_{CM}(\omega_c)]$ becomes null and the DEP force dies out. The dielectric characteristics of cells are well described by the single-shell model as detailed in our previous work.[2]

Hydrodynamic drag force acting on a cell, assuming a rigid particle, traveling in a viscous fluid at a relatively low speed is given by the Stoke's drag equation:

$$\bar{F}_{drag} = 6\pi\eta(\bar{u}_m - \bar{u}_c)R \quad \text{(S–3)}$$

where η is the dynamic viscosity of the fluid, and $\bar{u}_m$ and $\bar{u}_c$ are the velocity vectors of the fluid and the cell, respectively.

Cells railing reach a terminal velocity when there is no net force acting on them, including the friction along the tracks. The friction force, $\bar{F}_f$, is given by the relation $\bar{F}_f = \mu\bar{F}_N$, with μ the friction coefficient of the cell-track interface and $\bar{F}_N$ the surface-normal force exerted on the interface, which is mainly contributed by the DEP force.

SIMULATIONS

Simulations were performed on a 3D device model using COMSOL Multiphysics Software v4.3 (Comsol Inc., Burlington, MA). For the model, a scaled version of the flow chamber (the width and length) was built. The features of the electrode digit were kept as per the device (26° design), including the digit 3D profile, spacing, and dimensions (except for the digit length and count). This dimensional scaling was applied to ease the required computing budget. Figures S-1 and S-2 further illustrate the model and the meshing used whereas Tables S-1 and S-2 list the material characteristics and boundary conditions applied in the simulations, respectively.

The electric field distribution, $\bar{E}$, was obtained from the potential distribution ϕ, both solved for the model, using boundary conditions and the relations $\bar{E} = -\nabla\phi$, and $\nabla(\tilde{\sigma}_i\nabla\phi) = 0$. For a material denoted by the subscript i at a coordinate of interest, the complex conductivity, $\tilde{\sigma}_i$, relates to the electrical conductivity, σ_i, as well as permittivity, ε_i, through $\tilde{\sigma}_i = \sigma_i + j\omega\varepsilon_i$, where ω is the activation angular frequency and the complex $j = \sqrt{-1}$. Substituting $\bar{E}$ in eq (S–1), the time-averaged DEP force, $\langle\bar{F}_{DEP}\rangle$, was obtained across the model for a cell (diameter $R = 14$ μm) suspended in DEP buffer (the absolute permittivity $\varepsilon_m = 80\varepsilon_0$, with ε_0 being the

free-space permittivity $\varepsilon_0 = 8.854\times10^{-12}$ F/m). The value of $\mathrm{Re}[f_{CM}(\omega)]$ was taken as 0.95 as per the single-shell model[3] for an activation frequency of 400 kHz.

The flow velocity field $\bar{u}_m$ was obtained by solving Navier-Stokes equation for the model for an incompressible laminar flow. The inlet boundary was set at a constant velocity that corresponds to the sum of the sample and sheath flow rates stated in Figure 1 (0.85 mL/h). Maximum possible hydrodynamic force on the cell was considered assuming the cell stationary, $\bar{u}_c = 0$, in the Stokes' drag equation, i.e., $\bar{F}_{drag} = 6\pi\eta R\bar{u}_m$.

MOVIE

A binary mixture of 10-μm fluorescent polystyrene beads (Bangs Laboratories, Fishers, IN) and human colorectal carcinoma cells (HCT116; stained green) is shown flowing through the device (26° design) before and after the voltage activation onset. Before the voltage onset, the cells and beads can be seen moving through the passages beneath the tracks while being confined to the side of the chamber by the sheath flow leading them to the outlet I. After the voltage onset, the cells are seen being docked and railed along the tracks under pDEP, crossing the chamber and leaving through the outlet II whereas the beads under nDEP are seen proceeding to the outlet I. The movie corresponds to Figure 1. Sample flow: 0.5 mL/h. Each sample flanked by sheath flows I and II: 0.05 and 0.3 mL/h, respectively. Activation: 10 V_p applied at 400 kHz. DEP buffer: 100 μS/cm.

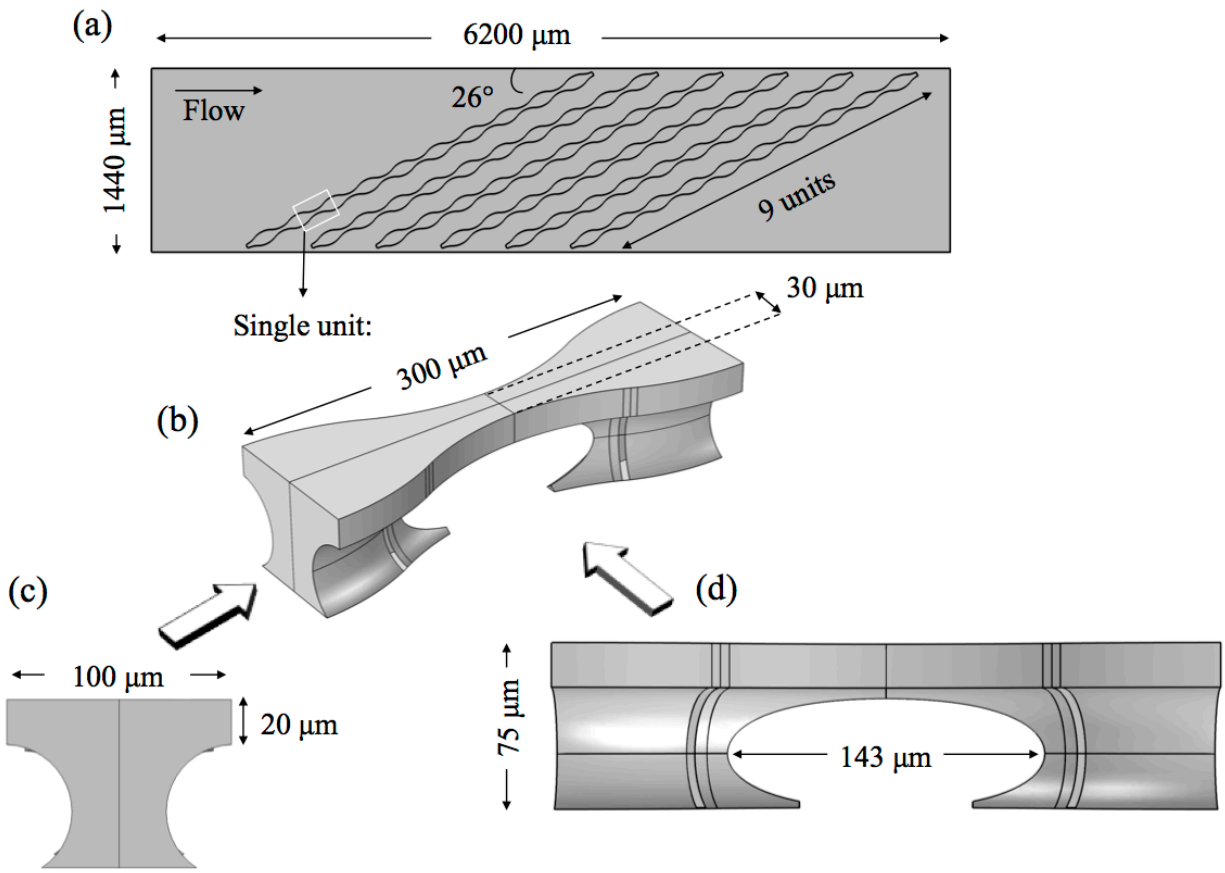

Figure S-1. The 3D device model simulated for the electric and flow velocity field, as well as the net force field distributions (considered only dielectrophoretic force and drag on a 14 µm cell). (a) Planar view of the flow chamber featuring three pairs of electrode digits, each having 9 units; (b-d) A single unit of an electrode digit described in (b) an isometric view, and (c,d) cross-sectional views as pointed out by the block arrows. The model corresponds to a scaled version of the flow chamber and retains all the other device dimensions as indicated above.

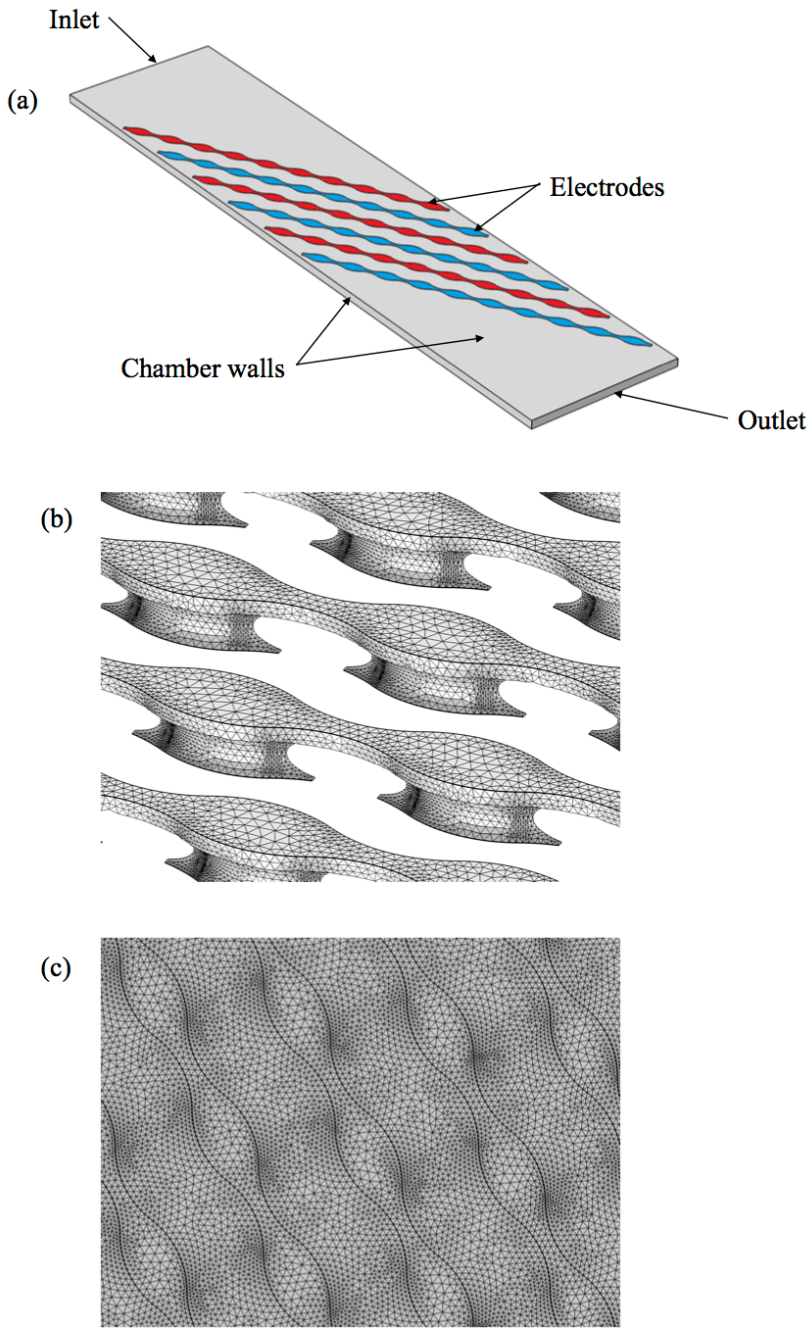

Figure S-2: (a) Model boundaries for which the conditions are set in the simulations (Table S-2). (b,c) Typical distributions of the mesh elements used in the simulations shown for the sections of the model: (b) the electrode digits and (c) the flow chamber. In total, 6.81×10^6 tetrahedral elements and 5.40×10^5 prism elements were used with the sizes refined to ensure the mesh-independency of the results.

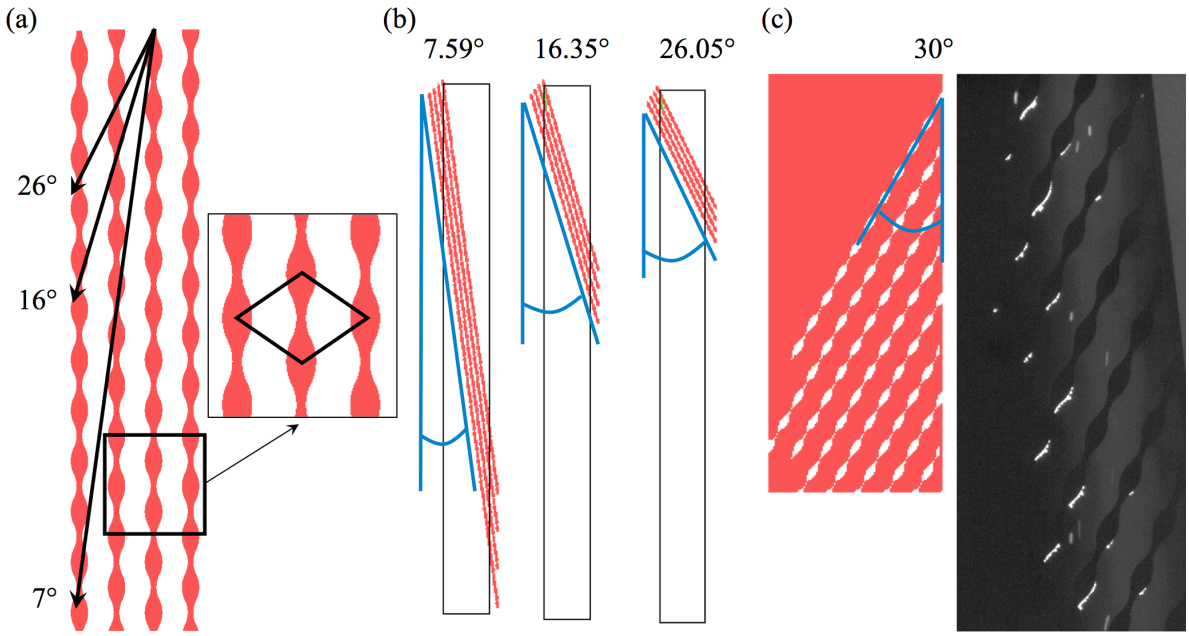

Figure S-3: Layout schematics of the electrode digits and the setting of the design (track) angle. (a) The columns supporting the tracks are arranged in a quadrilateral formation (inset) with all the dimensions fixed at the stated values across the designs regardless of the angle setting. The angle is set such that the corresponding passages beneath the tracks are aligned to maintain relatively straight streamlines (solid arrows). This restriction has limited the possible angle settings as can be noticed from the exact values displayed in (b). (c) The layout for 30° design and the corresponding image showing a typical unsuccessful case encountered often: HCT116 cells being held strongly along the tracks until their release without railing despite the gradually increased flow rate and reduced voltage. This design features a mirrored track direction compared to others.

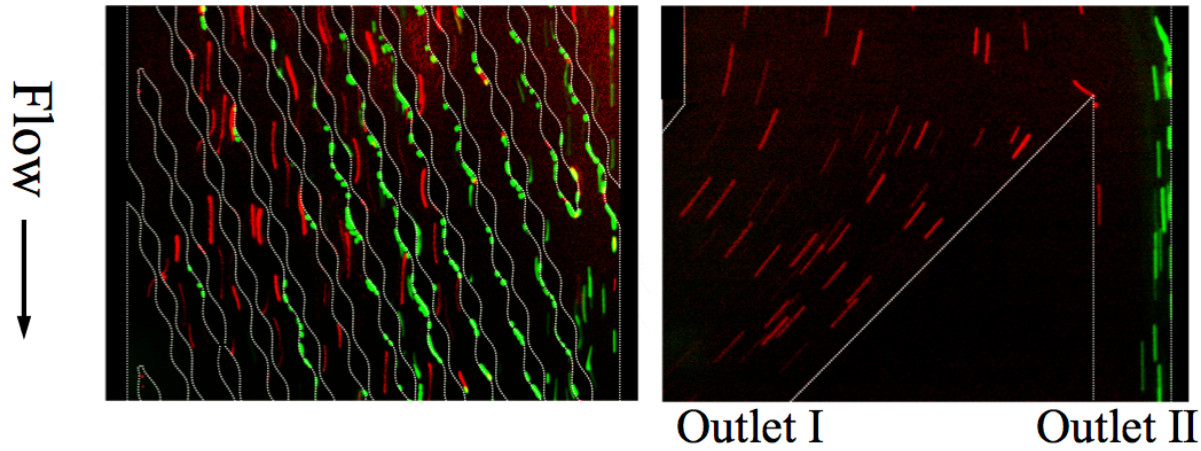

Figure S-4: Fluorescent micrographs of a section of the flow chamber and the device outlets captured during the sorting of HCT116 cells (green) and K562 cells (red) by having HCT116 cells railed along the tracks. These images correspond to Figure 6. Sample flow: 0.5 mL/h. Sheath flows: 0.05 and 0.3 mL/h. Activation: 12.5 V_p at 200 kHz. DEP buffer: 200 μS/cm.

Table S-1. Material characteristics used in the simulations.

Characteristic	**Silicon**	**DEP buffer**
Conductivity (S/m)	10^5	0.01
Relative permittivity	11.7	80
Dynamic viscosity (Pa s)	—	0.001
Density (kg/m^3)	—	1000

Table S-2. Boundary conditions set for the surfaces indicated in Figure S-2a.

Boundary	**Electric**[#]	**Fluidic**[*]
Red digits	Constant potential, $\phi = 7.5$ V$_p$	No slip, $\bar{u}_m = 0$
Blue digits	Ground potential	No slip, $\bar{u}_m = 0$
Inlet	Insulation, $\bar{n} \cdot \bar{\bar{E}} = 0$	$\bar{u}_m = 1.34$ mm/s
Outlet	Insulation, $\bar{n} \cdot \bar{\bar{E}} = 0$	$P_o = 1$ atm
Chamber walls	Insulation, $\bar{n} \cdot \bar{\bar{E}} = 0$	No slip, $\bar{u}_m = 0$

[#]The symbol $\bar{n}$ represents the surface normal vector.

[*]The symbol P_o represents the pressure at the outlet.

REFERENCES

(1) H. A. Pohl, Dielectrophoresis: The behavior of neutral matter in nonuniform electric fields, Cambridge University Press, 1978.

(2) X. Xing, R. Y. Poon, C. S. Wong and L. Yobas, *Biosens. Bioelectron.*, 2014, **61**, 434-442.

(3) X. Xing and L. Yobas, *Analyst*, 2015, **140**, 3397-3405.